

# UCSF

## UC San Francisco Previously Published Works

### Title

Factors Affecting Image Quality and Lesion Evaluability in Breast Diffusion-weighted MRI: Observations from the ECOG-ACRIN Cancer Research Group Multisite Trial (A6702)

### Permalink

<https://escholarship.org/uc/item/52f718p7>

### Journal

Journal of Breast Imaging, 3(1)

### ISSN

2631-6110

### Authors

Whisenant, Jennifer G  
Romanoff, Justin  
Rahbar, Habib  
[et al.](#)

### Publication Date

2021-01-26

### DOI

10.1093/jbi/wbaa103

Peer reviewed



Original Research

# Factors Affecting Image Quality and Lesion Evaluability in Breast Diffusion-weighted MRI: Observations from the ECOG-ACRIN Cancer Research Group Multisite Trial (A6702)

Jennifer G. Whisenant, PhD,<sup>1,2</sup> Justin Romanoff, MA,<sup>3</sup> Habib Rahbar, MD,<sup>4,6</sup> Averil E. Kitsch, BS,<sup>4</sup> Sara M. Harvey, MD,<sup>5</sup> Linda Moy, MD,<sup>6,9</sup> Wendy B. DeMartini, MD,<sup>7</sup> Basak E. Dogan, MD,<sup>8,9</sup> Wei T. Yang, MD,<sup>9</sup> Lilian C. Wang, MD,<sup>10</sup> Bonnie N. Joe, MD, PhD,<sup>11</sup> Lisa J. Wilmes, PhD,<sup>11</sup> Nola M. Hylton, PhD,<sup>11</sup> Karen Y. Oh, MD,<sup>12</sup> Luminita A. Tudorica, PhD,<sup>12</sup> Colleen H. Neal, MD,<sup>13</sup> Dariya I. Malyarenko, PhD,<sup>13</sup> Elizabeth S. McDonald, MD, PhD,<sup>14</sup> Christopher E. Comstock, MD,<sup>15</sup> Thomas E. Yankeelov, PhD,<sup>16</sup> Thomas L. Chenevert, PhD,<sup>13</sup> Savannah C. Partridge, PhD<sup>4,\*</sup>

<sup>1</sup>Vanderbilt University Medical Center, Department of Medicine, Nashville, TN; <sup>2</sup>Vanderbilt-Ingram Cancer Center, Nashville, TN; <sup>3</sup>Brown University, Center for Statistical Sciences, Providence, RI; <sup>4</sup>University of Washington, Department of Radiology, Seattle, WA; <sup>5</sup>Vanderbilt University Medical Center, Department of Radiology and Radiological Sciences, Nashville, TN; <sup>6</sup>New York University School of Medicine, Department of Radiology, New York, NY; <sup>7</sup>Stanford University School of Medicine, Department of Radiology, Stanford, CA; <sup>8</sup>University of Texas Southwestern Medical Center, Department of Diagnostic Radiology, Dallas, TX; <sup>9</sup>MD Anderson Cancer Center, Department of Breast Imaging, Houston, TX; <sup>10</sup>Northwestern University Feinberg School of Medicine, Department of Radiology, Chicago, IL; <sup>11</sup>University of California San Francisco School of Medicine, Department of Radiology and Biomedical Engineering, San Francisco, CA; <sup>12</sup>Oregon Health and Science University, Department of Radiology, Portland, OR; <sup>13</sup>University of Michigan, Department of Radiology/MRI, Ann Arbor, MI; <sup>14</sup>University of Pennsylvania Perelman School of Medicine, Department of Radiology, Philadelphia, PA; <sup>15</sup>Memorial Sloan-Kettering Cancer Center, Department of Radiology, New York, NY; <sup>16</sup>University of Texas Austin, Department of Biomedical Engineering, Austin, TX

\*Address correspondence to S.C.P. (e-mail: [scp3@uw.edu](mailto:scp3@uw.edu))

## Abstract

**Objective:** The A6702 multisite trial confirmed that apparent diffusion coefficient (ADC) measures can improve breast MRI accuracy and reduce unnecessary biopsies, but also found that technical issues rendered many lesions non-evaluable on diffusion-weighted imaging (DWI). This secondary analysis investigated factors affecting lesion evaluability and impact on diagnostic performance.

**Methods:** The A6702 protocol was IRB-approved at 10 institutions; participants provided informed consent. In total, 103 women with 142 MRI-detected breast lesions (BI-RADS assessment category 3, 4, or 5) completed the study. DWI was acquired at 1.5T and 3T using a four *b*-value, echo-planar imaging sequence. Scans were reviewed for multiple quality factors (artifacts, signal-to-noise, misregistration, and fat suppression); lesions were considered non-evaluable if there was low confidence in ADC measurement. Associations of lesion evaluability with imaging and lesion

characteristics were determined. Areas under the receiver operating characteristic curves (AUCs) were compared using bootstrapping.

**Results:** Thirty percent (42/142) of lesions were non-evaluable on DWI; 23% (32/142) with image quality issues, 7% (10/142) with conspicuity and/or localization issues. Misregistration was the only factor associated with non-evaluability ( $P = 0.001$ ). Smaller ( $\leq 10$  mm) lesions were more commonly non-evaluable than larger lesions ( $p < 0.03$ ), though not significant after multiplicity correction. The AUC for differentiating benign and malignant lesions increased after excluding non-evaluable lesions, from 0.61 (95% CI: 0.50–0.71) to 0.75 (95% CI: 0.65–0.84).

**Conclusion:** Image quality remains a technical challenge in breast DWI, particularly for smaller lesions. Protocol optimization and advanced acquisition and post-processing techniques would help to improve clinical utility.

**Key words:** multicenter trial; breast magnetic resonance imaging (MRI); apparent diffusion coefficient (ADC); artifacts; diagnostic performance.

#### Key Messages

- Qualitative assessment of the A6702 imaging data demonstrated that 30% (42/142) of MRI-detected breast lesions were deemed non-evaluable due to variable technical issues relating to both image quality and spatial resolution on diffusion-weighted imaging.
- Misregistration of images within the diffusion-weighted imaging series (due to patient motion and/or eddy current effects) was the factor most associated with lesion non-evaluability ( $P = 0.001$ ).
- Diagnostic performance of diffusion-weighted imaging was higher when only considering those lesions deemed evaluable (area under the curve = 0.75 versus 0.61 for those deemed non-evaluable).

## Introduction

MRI is a highly sensitive method for the detection of breast cancer and is increasingly being used as a screening tool in conjunction with mammography, especially in high-risk women (1). Despite the high sensitivity, many benign lesions cannot be distinguished from malignant ones based solely on contrast-enhanced MRI features (including both morphology and kinetics), resulting in limited positive predictive value and unnecessary biopsies (2). Diffusion-weighted imaging (DWI) holds potential as a complementary technique to conventional contrast-enhanced breast MRI to improve diagnostic accuracy. DWI characterizes the mobility of water molecules in tissues, which can be quantified by the apparent diffusion coefficient (ADC). Several *in vivo* studies have shown that tissue areas of higher cellularity, such as tumors, often exhibit lower ADCs (3–6). Because malignant lesions typically have higher cellular density than benign lesions, there have been numerous investigations of the utility of ADC to differentiate breast lesions and potentially stratify grades of malignancy (3,7,8). Although multiple single-institution studies have shown promising results that

suggest DWI improves the specificity of contrast-enhanced breast MRI (9–13), DWI and/or ADC measurement has not been incorporated into the standard Breast Imaging Reporting and Data System (BI-RADS) recommendations (14). Multiple factors have limited clinical adoption, including lack of standardized protocols, variance between reported optimal diagnostic ADC thresholds, unclear performance in clinically relevant lesion subgroups (e.g. non-masses and small lesions with diameters  $< 10$ – $12$  mm), and scan time constraints.

Given the promise of DWI to improve the diagnostic accuracy of breast MRI, the Eastern Cooperative Oncology Group—American College of Radiology Imaging Network (ECOG-ACRIN) Cancer Research Group performed the A6702 phase II multicenter trial to confirm ADC differences between benign and malignant lesions across multiple MRI systems and practice sites, and to identify an ADC threshold to reduce the biopsy rate of benign lesions that could be further explored in future phase III trials (15). Results of the trial confirmed that ADC measures could reduce the rate of false positive findings of malignancy breast MRI across practice sites and potentially lower the overall biopsy rate by 20%–26%, but it was also found that DWI had some challenging technical issues. Almost one-third of the MRI-detected lesions could not be evaluated with confidence on DWI due to various technical factors, and were subsequently excluded. Thus, the purpose of this secondary analysis was to identify factors affecting lesion evaluability in the A6702 trial and to assess the impact of image quality on the diagnostic performance of breast DWI.

## Methods

### Study Participants

Between January 2014 and April 2015, women aged 18 years and older undergoing a breast MRI examination for any clinical indication provided written informed consent to undergo a study-specific DWI sequence during their examination to participate in the A6702 trial. The internal review boards of the 10 participating institutions reviewed and approved the

study protocol. The study was compliant with the Health Insurance Portability and Accountability Act.

All breast MRIs were interpreted using the non-DWI sequences (e.g. pre-contrast and gadolinium contrast-enhanced T1-weighted images and T2-weighted images) in accordance with each institution's standard of care and American College of Radiology accreditation guidelines. Those women with at least one BI-RADS assessment category 3 (probably benign), 4 (suspicious for malignancy), or 5 (highly suggestive of malignancy) lesion were enrolled in the study. Target enrollment for the trial (ClinicalTrials.gov identifier: NCT02022579) was 100 subjects. To reduce bias from performance at any one institution, maximal accrual at each site was capped at 40 study participants. Participants who received neoadjuvant chemotherapy between the MRI examination date and pathological assessment of the lesion were excluded. Additional eligibility criteria and reference standard methodology are described in a recent publication (15). The management of individual lesions was based on institutional standard of care guidelines, with the expectation that all participants would either undergo a lesion biopsy following the study MRI (for BI-RADS category 4 or 5 lesions) or imaging and/or clinical follow-up at six-month intervals (for BI-RADS category 3 lesions).

### Reference Standard for Lesion Outcome

The reference standard for each breast lesion was determined from the results of the image-guided biopsy, surgery, or follow-up MRI exams at 12 months (if applicable). The reference standard was considered to be indeterminate for BI-RADS category 4 or 5 lesions if no sampling of the lesion was performed and there was no follow-up MRI that downgraded the initial finding. Additionally, the reference standard for category 4 or 5 lesions that were excised during surgery for another lesion (e.g. an ipsilateral cancer) without prior sampling was also considered indeterminate.

### DWI Acquisition

Imaging was performed on 1.5T or 3T MRI scanners using a dedicated breast radiofrequency coil with a conventional dynamic contrast-enhanced (DCE) breast sequence acquired in accordance with each institution's standard of care and American College of Radiology accreditation guidelines. Each site performed a standardized DWI protocol prior to contrast injection using a commercially available diffusion-weighted, single-shot, spin-echo, echo-planar imaging (EPI) sequence; standardized scan parameters are listed in Table 1. The DWI protocol utilized in the A6702 trial aligns well with the recent consensus recommendations from the European Society of Breast Imaging (16) and the DWI profile published by the Quantitative Imaging Biomarkers Alliance (17). Due to limited availability across scanner platforms, image registration was not incorporated as part of the acquisition protocol for the study.

Each MRI system utilized in this study was required to first pass a DWI qualification process, incorporating

**Table 1.** Breast Diffusion-weighted Imaging Acquisition Parameters

Parameter	Diffusion-weighted Imaging
Sequence type	Diffusion-weighted, single-shot, spin echo, echo-planar imaging
2D or 3D sequence	2D
Fat suppression	Active fat-saturation
Laterality	Bilateral
Phase direction	Anterior-to-posterior (right-to-left optional)
In-plane resolution	1.5–2.0 mm
Field of view	36 cm (optional) <sup>a</sup>
Acquisition matrix	Variable, depending on field of view
Reconstruction matrix	256 × 256
Slice thickness (acquired)	4 mm
Slice gap	No gap
Number of slices	Acquire the maximum number that can be acquired in a single acquisition (typically 24–30 slices)
Repetition time	≥4000 ms
Echo time	Minimum (50–100 ms)
Bandwidth (water–fat shift)	Maximum (water–fat shift = minimum)
Flip angle	90°C
<i>b</i> -values	0, 100, 600, 800 s/mm <sup>2</sup>
Number of gradient directions	3 orthogonal axes
Parallel imaging factor	≥2
Number of excitations/averages	≥2
Sequence acquisition time	Approximately 5 minutes

<sup>a</sup>Set field of view based on body habitus to include both breasts and axilla and to avoid wrap artifacts.

assessment of both phantom and patient studies (18). DWI qualification included a central review of test scans in temperature-controlled phantoms (19) to quantify system ADC bias and uniformity, relative signal-to-noise, and scan protocol compliance. Representative patient scans from each site were also reviewed to verify acceptably low artifact level, adequate signal-to-noise, and homogeneous fat suppression (15). In addition, regular DWI quality control scans were performed every six months for each site, as well as after any major scanner system software upgrade or change in breast coil.

### ADC Measurements

Centralized analysis was performed to obtain consistent tumor ADC measures for all lesions in the trial. Custom software built in MATLAB (version 2015a, The MathWorks, Natick, MA) was used to calculate ADC maps using a mono-exponential decay model (20) with linear least squares fitting of the signal decay with increasing *b*-value. Centralized lesion



regions of interest (ROIs) were manually defined by trained research scientists at the University of Washington under the supervision of the co-chairs of the study (H.R. and S.C.P.), who were blinded to the lesion outcomes. Briefly, lesions were located on the diffusion-weighted images by cross-referencing appearance on conventional contrast-enhanced images and to assist in avoiding adjacent normal fibroglandular or adipose tissue. Whole-lesion (ie, multi-slice) ROIs were then drawn on the diffusion-weighted images with the assistance of a semiautomated thresholding tool (21) to further prevent the inclusion of non-lesion tissue. ROIs were propagated to the ADC maps, and the mean ADC within the lesion ROI was calculated.

### DWI Quality and Lesion Evaluability

During centralized analysis, image quality and lesion evaluability were assessed qualitatively by a single trained research scientist (A.E.K.) in consultation with two expert investigators with more than 15 (S.C.P.; quantitative imaging scientist) and seven (H.R.; clinical breast radiologist) years of breast DWI experience. All reviewers were blinded to lesion pathologic outcomes. Image quality factors relating to inadequate fat suppression, signal-to-noise ratio (SNR), image artifacts (magnetic susceptibility distortion, aliasing, and chemical shift), and misregistration within DWI series were reviewed. A lesion ROI was attempted in all cases, regardless of image quality, but lesions for which reviewers had low confidence with the ADC measurement due to substantial issues with DWI quality and/or lesion ROI delineation were categorized as non-evaluable for analysis purposes. Challenges with ROI delineation could have resulted from the presence of image quality issues, partial volume averaging, or limited lesion contrast with respect to the surrounding non-lesion tissue. It should be noted that it was possible for a patient to have one lesion that was evaluable and another lesion that was non-evaluable, depending on lesion characteristics and image quality factors local to the lesion in question.

### Statistical Analysis

Participant and lesion characteristics were summarized as either median and range (for continuous features) or by counts and percentages (for categorical features). To test the relationship between exam and/or imaging features and lesion evaluability, we regressed the lesion evaluability on each covariate of interest using logistic regression models with generalized estimating equations and an exchangeable working correlation structure to account for within-patient correlation between lesions. Each *P* value is from a generalized Wald test for which the coefficient of the covariate of interest was equal to zero. Comparisons between quality factors and MRI field strength and vendor were performed using Fisher's exact test.

The areas under the receiver operating characteristic (ROC) curves (AUCs) were calculated empirically at the lesion-level using centrally reviewed ADC measures to assess

diagnostic performance and their 95% confidence intervals (CIs) were computed using bootstrapping (22). Participants were stratified by their reference standard (any malignant lesion or no malignant lesions) and were sampled with replacement within each stratum. The AUC was evaluated within each resampled dataset, and the standard error of the bootstrapped AUCs was used to calculate the 95% CI under the assumption of normality.

All reported *P* values are unadjusted and obtained from two-sided tests. Multiplicity was controlled for post hoc using a Bonferroni correction. In total, 21 comparisons were made, and therefore a *P* value of <0.003 was required to conclude statistical significance. Statistical analyses were performed using SAS/STAT (version 9.4, SAS Institute Inc., Cary, NC) and R (version 3.6.2, R Foundation for Statistical Computing, Vienna, Austria).

## Results

### Patient and Exam Characteristics

Between January 2014 and April 2015, 1002 women from 10 academic institutions consented to participate in the trial prior to undergoing a breast MRI. A total of 107 women had at least one lesion categorized with a BI-RADS 3, 4, or 5 assessment and were enrolled. Four subjects were subsequently

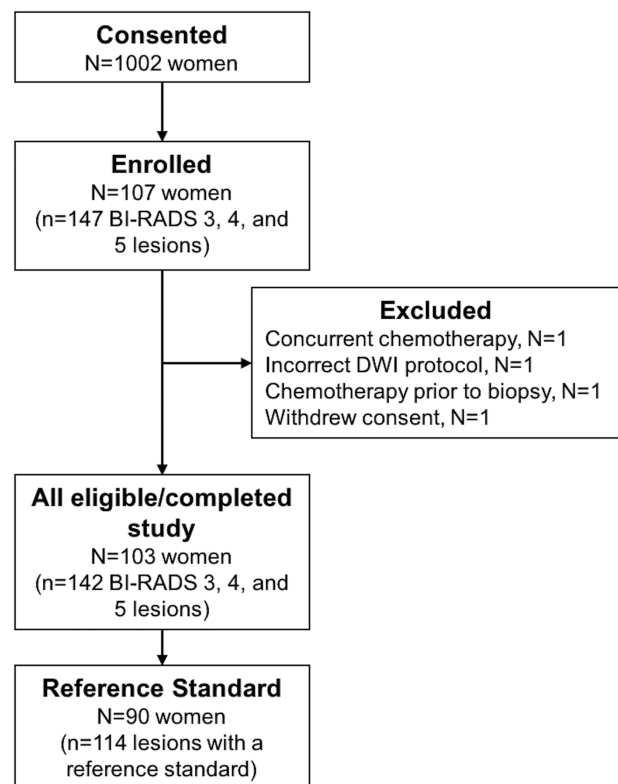


**Figure 1.** ECOG-ACRIN A6702 trial participant and image quality analysis flowchart. Abbreviations: DWI, diffusion-weighted imaging; ECOG-ACRIN, Eastern Cooperative Oncology Group—American College of Radiology Imaging Network.

excluded due to concurrent chemotherapy, incorrect DWI acquisition protocol, receipt of chemotherapy prior to lesion biopsy, and withdrawal of consent, resulting in 103 women with 142 lesions completing the study (Figure 1). Of those, a reference standard to determine benign or malignant lesion outcome was available for 114 lesions (80 benign, 34 malignant) in 90 women.

Patient and exam features are listed in Table 2. The median age for the 103 women was 47 years (range: 24–75 years), and the majority (59%, 61/103) of the DWI scans were performed at 3T. Multiple vendor platforms were represented, including Philips (Philips Healthcare, Best, Netherlands), Siemens (Siemens Healthineers, Erlangen, Germany), and GE (GE Healthcare, Waukesha, WI) systems at both 1.5T and 3T field strengths. Similar distributions were observed in the sub-cohort of participants that had a reference standard for at least one lesion (Table 2).

### Observed DWI Quality Issues

Inadequate fat suppression or SNR was noted as an image quality issue in 24% (25/103) and 20% (21/103) of DWI scans, respectively; magnetic susceptibility artifacts were noted in 19% (20/103); aliasing artifacts were noted in 11% (11/103); and misregistration was noted in 20% (21/103) (Table 3). Presence of SNR issues and aliasing artifacts

varied significantly with scanner vendor ( $P < 0.001$  for both). Exams at 1.5T were more prone to misregistration than 3T exams (36% (15/42) versus 10% (6/61);  $P = 0.002$ ), while 3T exams more often exhibited aliasing artifacts than 1.5T exams (18% (11/61) versus 0% (0/42);  $P = 0.003$ , but not significant after adjustment for multiplicity). A representative evaluable exam with good DWI quality (i.e. no issues identified) is presented in Figure 2, while various examples of specific quality issues encountered in the trial are highlighted in Figures 3–7. Figure 3 displays a representative example of poor fat suppression, while Figure 4 presents a typical DWI aliasing artifact. Figures 5 and 6 highlight representative examples of low SNR and spatial distortion, respectively. Figure 7 presents a representative example of misregistration.

### Factors Associated with Lesion Non-evaluability

Table 4 summarizes characteristics of all lesions included in the study and the image quality factors noted. Of the 142 lesions, 30 were BI-RADS category 3, 105 were category 4, and 7 were category 5. A majority (57%, 81/142) of lesions were  $\leq 10$  mm in diameter, and masses were the most common finding (51%, 73/142).

In total, 30% (42/142) of lesions were considered non-evaluable from 35 women, of which 5 women had 2 non-evaluable lesions and 1 had 3 non-evaluable lesions; 8 women also had another lesion that was evaluable. In terms of lesion characteristics, smaller ( $\leq 10$  mm;  $n = 81$ ) lesions were more commonly non-evaluable than larger lesions, although this was not significant after adjustment for multiple comparisons ( $P = 0.030$ ; Table 4). Lesion morphology (mass, non-mass enhancement, or focus) and BI-RADS score were not associated with lesion evaluability ( $P = 0.247$  and  $P = 0.978$ , respectively). In terms of image quality factors, 32/42 (76%) non-evaluable lesions were observed to have image quality issues, with 19/42 (45%) demonstrating multiple image quality issues. Misregistration (attributed to patient motion or eddy currents) was significantly associated with lesion non-evaluability ( $P = 0.001$ ), while inadequate fat suppression and SNR, and the presence of magnetic susceptibility and aliasing artifacts, were not ( $P = 0.732$ ,  $P = 0.081$ ,  $P = 0.717$ , and  $P = 0.162$ , respectively). Neither MRI system vendor nor field strength were significantly associated with lesion evaluability ( $P = 0.297$  and  $P = 0.953$ , respectively) (Table 4).

Ten lesions were considered non-evaluable for reasons other than image quality issues: 1 lesion was located outside of the DWI slice coverage area, and the other 9 lesions were not visible on DWI and were difficult to confidently localize and define an ROI for due to limited anatomical agreement between DCE and DWI. Those 9 lesions were typically composed of small, scattered foci or diffuse lesions within heterogeneous breast tissue. This issue highlights the fact that lesions can still be non-evaluable with DWI even if the image quality is sufficient, due to the nature of some breast lesions and suboptimal spatial resolution.

**Table 2.** Participant and Exam Features

	All Eligible Participants ( <i>N</i> = 103)	Participants with a Reference Standard ( <i>N</i> = 90)
	<i>n</i> (%)	<i>n</i> (%)
Patient age		
<50 years	57 (55)	47 (52)
$\geq 50$ years	46 (45)	43 (48)
Clinical indication for MRI		
Known breast cancer	45 (44)	42 (47)
Screening	29 (28)	23 (26)
Short-interval follow-up	6 (6)	6 (7)
Other/multiple	23 (22)	19 (21)
Number of study lesions per patient		
1	75 (73)	73 (81)
2	19 (18)	11 (12)
3	7 (7)	5 (6)
4	2 (2)	1 (1)
MRI vendor		
Philips	63 (61)	58 (64)
Siemens	21 (20)	17 (19)
GE	19 (18)	15 (17)
MRI field strength		
1.5 T	42 (41)	38 (42)
3.0 T	61 (59)	52 (58)

**Table 3.** Image Quality Factors Stratified by MRI Vendor and Field Strength

	MRI Vendor				P Value	MRI Field Strength		P Value
	Total (N = 103)	Philips (N = 63)	Siemens (N = 21)	GE (N = 19)		1.5T (N = 42)	3.0T (N = 61)	
	n (%)	n (%)	n (%)	n (%)		n (%)	n (%)	
Fat suppression issue					0.218			0.816
No	78 (76)	47 (75)	14 (67)	17 (89)		31 (74)	47 (77)	
Yes	25 (24)	16 (25)	7 (33)	2 (11)		11 (26)	14 (23)	
Signal-to-noise ratio issue					<0.001 <sup>a</sup>			1.000
No	82 (80)	59 (94)	8 (38)	15 (79)		33 (79)	49 (80)	
Yes	21 (20)	4 (6)	13 (62)	4 (21)		9 (21)	12 (20)	
Magnetic susceptibility artifact					1.000			0.075
No	83 (81)	51 (81)	17 (81)	15 (79)		30 (71)	53 (87)	
Yes	20 (19)	12 (19)	4 (19)	4 (21)		12 (29)	8 (13)	
Aliasing artifact					<0.001 <sup>a</sup>			0.003
No	92 (89)	63 (100)	11 (52)	18 (95)		42 (100)	50 (82)	
Yes	11 (11)	0 (0)	10 (48)	1 (5)		0 (0)	11 (18)	
Misregistration issue					0.014			0.002 <sup>a</sup>
No	82 (80)	46 (73)	21 (100)	15 (79)		27 (64)	55 (90)	
Yes	21 (20)	17 (27)	0 (0)	4 (21)		15 (36)	6 (10)	

<sup>a</sup>P value is significant after adjustment for multiple comparisons.

### Effect of Image Quality on Diagnostic Performance

For lesions with a reference standard (n = 114), ROC analysis was performed to estimate the ability of ADC values to discriminate between benign and malignant lesions (Figure 8). First, considering all lesions, without regard to image quality (excluding the 1 lesion where ADC could not be measured because it was located outside the DWI slice coverage area; final n = 113 lesions), the estimated AUC was 0.61 (95% CI: 0.50–0.71). Next, ROC analysis was repeated considering only the evaluable (n = 81) lesions, and the estimated AUC increased to 0.75 (Figure 8; 95% CI: 0.65–0.84; P = 0.037).

### Discussion

The ECOG-ACRIN A6702 trial demonstrated the clinical utility of breast DWI to reduce the rate of unnecessary biopsy; however, the initial report from this study briefly highlighted that technical issues still plague DWI in the breast (15). The objectives of this study were to present a more comprehensive review of the technical challenges observed in the trial, including comparisons by vendor and field strength, identify factors associated with lesion evaluability, and evaluate the impact on diagnostic performance of breast DWI. In this secondary analysis, it was found that lesions deemed non-evaluable for ADC quantitation tended to be of smaller size ( $\leq 10$  mm) or to have an image quality issue. Conversely, lesion morphology (mass or non-mass), magnet field strength, and MRI vendor were not found to impact lesion evaluability. As noted earlier, 10 of the 42 non-evaluable

lesions were excluded due to reasons other than the presence of an image quality issue, most commonly when the lesion was not sufficiently visible to have confidence in the ROI placement. While image quality issues were observed in many examinations, for the majority of cases these were considered relatively minor or sufficiently distant from the lesion in question and were not deemed to render the lesion non-evaluable.

After correcting for multiple comparisons, spatial misregistration between diffusion-weighted images was the only image quality factor significantly associated with lesion evaluability (P = 0.001). Two sources of DWI misregistration are eddy currents induced during the application of strong diffusion gradients that cause additional image distortions in the direction of the applied gradients (23), and patient motion, which can result in misalignment between the diffusion-weighted images at each slice level and thus inaccuracies in the ADC map. Misregistration issues were observed more often with 1.5T scanners compared to 3.0T (P = 0.002), and varied somewhat with scanner vendor, which likely reflects different DWI sequence variants and acquisition parameter options available across systems. A twice-refocused diffusion preparation is one alternative acquisition strategy to reduce eddy currents in breast DWI (24). This preparation utilizes additional radiofrequency refocusing pulses that split the gradient pulses into shorter pulses of alternative polarity in order to eliminate specific exponentially decaying fields, such as those from eddy currents that decay slowly (25). Image registration post-processing techniques, which were not implemented for the

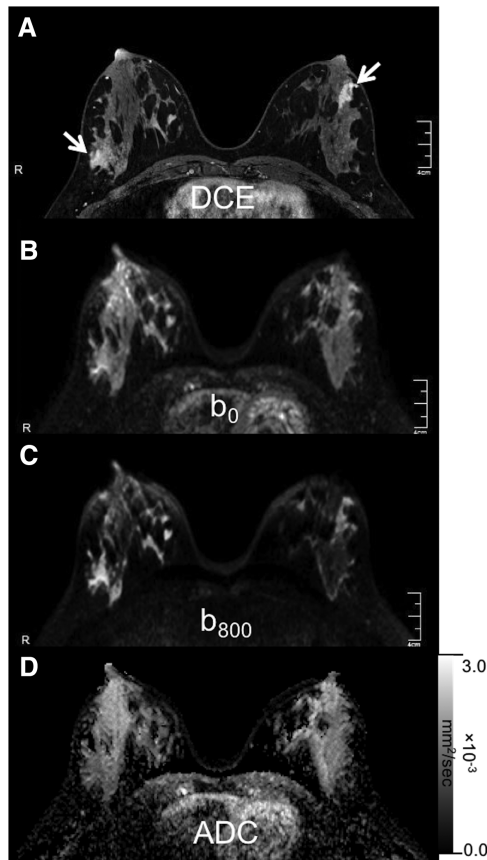


**Figure 2.** Example of a good-quality diffusion-weighted imaging (DWI) data set in a 37-year-old woman undergoing 3T MRI for high-risk screening. Dynamic contrast-enhanced (DCE) MRI (A) demonstrates bilateral segmental non-mass enhancement (arrows), each assessed as BI-RADS 3. Using the contrast-enhanced images for anatomical comparison, the DWI (B and C) and corresponding apparent diffusion coefficient (ADC) map (D) appear relatively undistorted, with sufficient signal-to-noise in fibroglandular tissue regions, even in the  $b = 800$  s/mm<sup>2</sup> image (C). Fat suppression is adequate, and no chemical shift or other artifacts are apparent to impair lesion visualization and ADC measurement.

A6702 centralized primary analysis, can also be used to reduce spatial misalignment and improve accuracy in the ADC measurement (26,27). However, a prior study reported that 11% of breast DWI exams had misalignment that could not be corrected using an image registration algorithm (13), emphasizing the importance of implementing corrective strategies to minimize subject motion and eddy current effects at the time of data acquisition. Reducing scan times and increasing patient comfort during the scan may help to minimize patient-related motion.

The presence of SNR issues and aliasing artifacts varied significantly between vendor; however, the cause is unknown and likely multifactorial. The impact of coil sensitivity, gradient performance, sequence variants, and poor shimming quality, as well as technologist experience and patient variation, could be factors associated with this

observation. These issues are something that would merit investigating in a larger dataset. Additionally, these results represent a snapshot of the available technology at the time, which is ever-evolving with newer hardware and software, as well as advanced sequences, and therefore may not be generalizable across MRI systems.

The DWI protocol in this trial employed a single-shot EPI-based sequence because of its wide cross-platform availability and ability to achieve very fast image acquisition to minimize motion artifacts. However, standard single-shot EPI in the breast is prone to multiple image artifacts that were observed in the trial, including those due to chemical shift, magnetic susceptibility, and gradient field eddy currents (23). This technique also provides limited spatial resolution for breast imaging due to the large field of view (FOV) needed for both breasts (to collect full bilateral coverage and avoid phase wrap) and restricted matrix sizes (required for short readout durations that offer sufficient SNR). Advanced acquisition and post-processing techniques hold promise to overcome many of the image quality issues of standard single-shot EPI for breast DWI. These include multi-shot (e.g. readout-segmented (28) and multiplexed sensitivity-encoding (29)) and reduced FOV (30) EPI techniques, each of which offer benefits of improved spatial resolution and reduced susceptibility artifacts by shortening echo spacing and/or echo train lengths. However, these advanced acquisition methods come at the expense of longer scan times and/or reduced coverage and are not yet widely implemented across different vendor platforms. Post-processing techniques have also been developed to mitigate EPI distortions from magnetic field inhomogeneity (31,32) and correct  $b$ -value inaccuracies due to gradient nonlinearities (33), which can further improve diffusion image quality and ADC accuracy.

In future trials, incorporating more immediate feedback to sites regarding image quality issues may decrease the rate of lesion non-evaluability, and onsite clinician and technologist training to identify more subtle DWI quality issues is important. Additionally, as advanced acquisition strategies and post-processing solutions become more readily available on clinical scanners and workstations, these techniques could increase image quality and thus potentially lower the number of non-evaluable lesions on breast DWI. It is important to note that utilization of ADC as a diagnostic marker to improve breast MRI specificity is analogous to DCE kinetics metrics, which have already been codified in the breast MRI BI-RADS atlas. Although known to improve differentiation between benign and malignant breast lesions, DCE kinetics have been shown to vary across MRI systems and acquisition protocols (34), and with lesion morphology (35,36), resulting in variable diagnostic performance. With improvements in DWI strategies, the robustness of ADC measures is likely to improve, and could also be easily implemented into abbreviated MRI protocols to replace missing kinetics information and retain specificity.



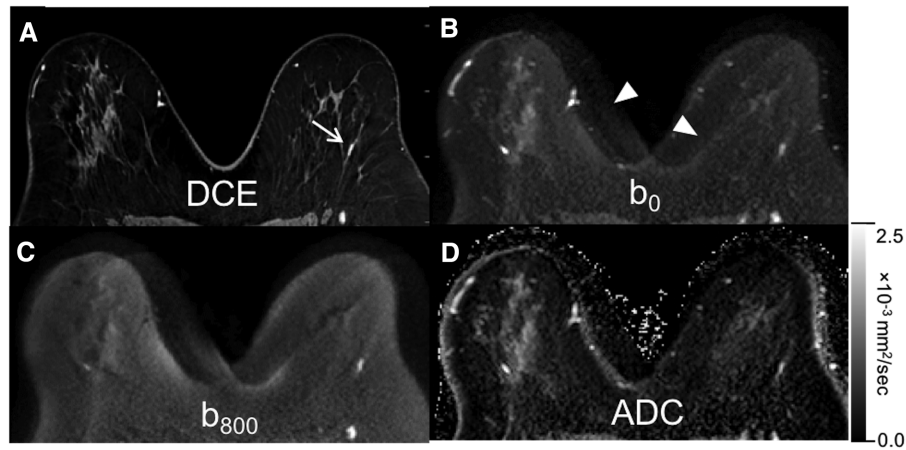


**Figure 3.** Example of poor fat suppression in a 53-year-old woman undergoing 1.5T MRI for high-risk screening. Dynamic contrast-enhanced (DCE) MRI (A) demonstrates a 9-mm area of linear non-mass enhancement in the left breast (arrow), assessed as BI-RADS category 3. On diffusion-weighted imaging (B and C), unsuppressed fat results in a chemical shift artifact of fat signal displaced (by a few centimeters in the right–left phase-encode direction) and overlaid on the image (arrowheads), thereby decreasing lesion visibility and artificially reducing the resulting lesion apparent diffusion coefficient (ADC) value (D). In this example, ADC values and lesion visibility on the ADC map are impacted due to poor fat suppression resulting in a more pronounced chemical shift artifact.

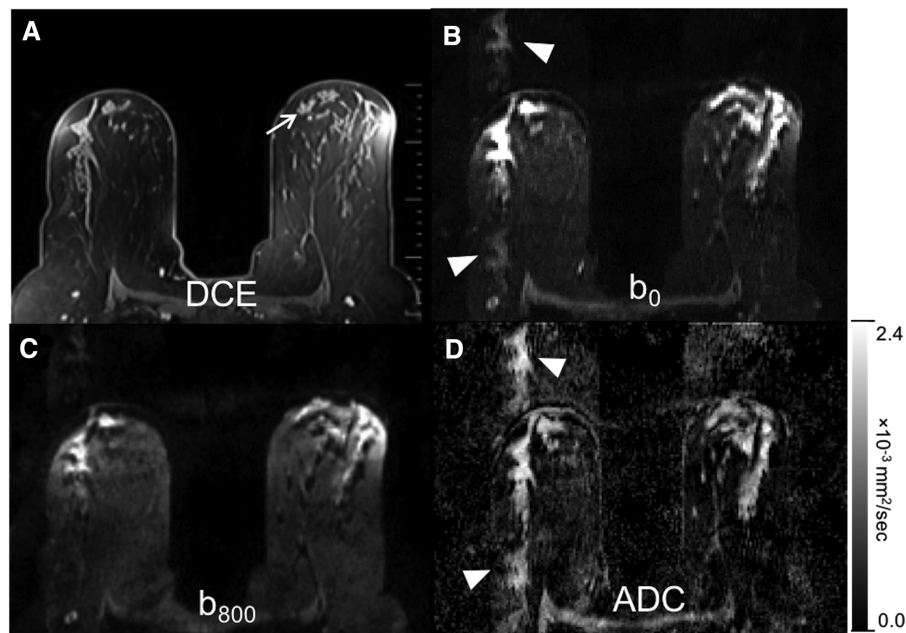


**Figure 4.** Example of diffusion-weighted imaging (DWI) data with aliasing, which can be identified by repeating parenchyma in the image along the phase encoding direction. Dynamic contrast-enhanced (DCE) MRI (A) in a 65-year-old woman undergoing 3T MRI for short-interval follow-up for bilateral BI-RADS category 3 enhancing foci, such as the one shown in the left breast (arrow). On DWI (B and C) and the apparent diffusion coefficient (ADC) map (D), repeated signal from the breast fibroglandular tissue is observed in the phase-encode (antero-posterior) direction, particularly across the right breast (B and C, arrowheads).

This study had several limitations. First, the A6702 trial was not powered for these secondary analyses and so sample sizes may be too low to identify significant factors affecting data quality. The findings associated with vendor and field strength could be influenced by site-specific protocol optimization and operator training rather than equipment.

Second, image quality factors and lesion evaluability were assessed qualitatively at the time of the primary centralized lesion ADC measurement, which may limit reproducibility of the findings. A future study to characterize image quality factors using more objective quantitative methods (e.g. five-point Likert scale (37), direct SNR calculations, distortion

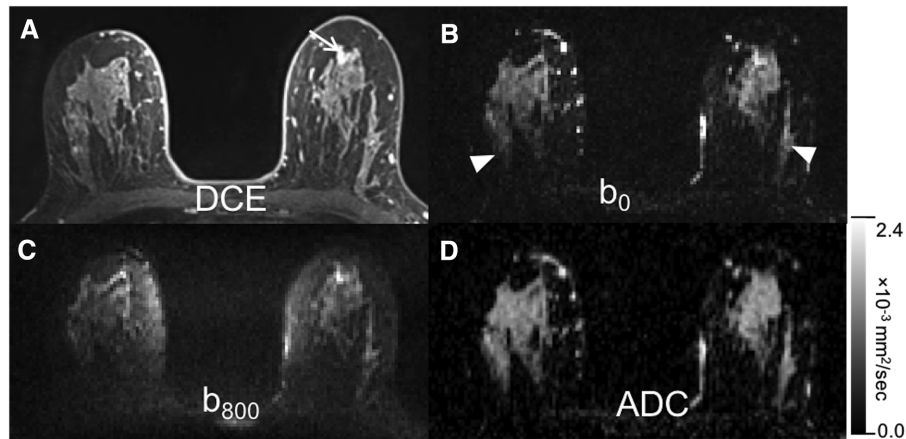


**Figure 5.** Diffusion-weighted imaging (DWI) dataset with poor signal-to-noise ratio (SNR) in a 43-year-old high-risk woman undergoing 1.5T MRI to evaluate extent of disease for a newly diagnosed breast cancer in the right breast (lesion not shown in images). Dynamic contrast-enhanced (DCE) MRI (A) demonstrates an 18-mm area of non-mass enhancement in the left breast (arrow), assessed as BI-RADS category 4. On DWI (B and C), poor SNR is apparent due to lack of definite tissue boundaries, even on the  $b_0$  image (B, arrowheads), and noisy apparent diffusion coefficient (ADC) map (D).

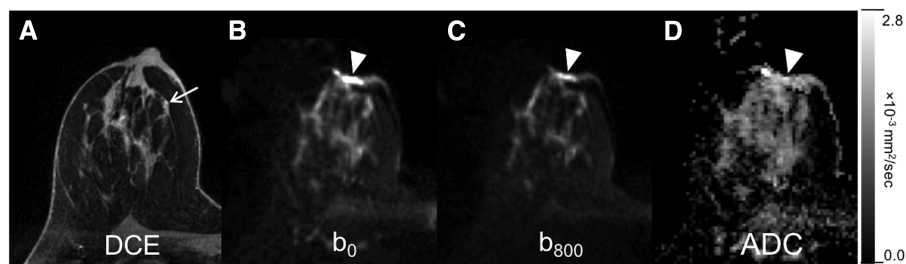


**Figure 6.** Example of spatial distortion artifact diffusion-weighted imaging (DWI) data set in a 55-year-old woman undergoing 3T MRI for high-risk screening due to personal history of breast cancer. Dynamic contrast-enhanced (DCE) MRI (A) demonstrates a subareolar region of non-mass enhancement in the right breast (arrow), assessed as BI-RADS category 4. In comparison, severe geometric distortion on DWI (B–D) is observed along the tissue-air interface at the nipple (arrowheads) caused by poor overall shim and/or local susceptibility gradients. Abbreviation: ADC, apparent diffusion coefficient.

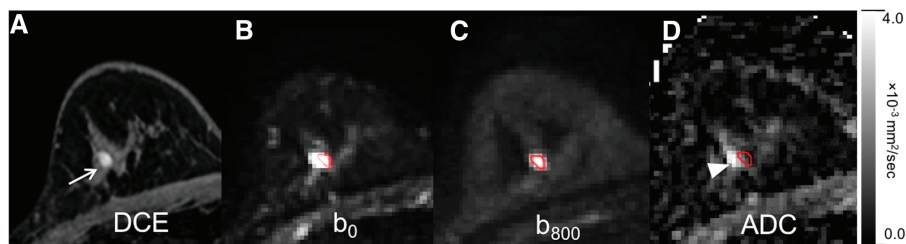


**Figure 7.** An example diffusion-weighted imaging (DWI) dataset exhibiting misregistration between the different  $b$ -values in a 51-year-old woman undergoing 1.5T MRI to evaluate extent of disease for a known cancer in the right breast. Dynamic contrast-enhanced (DCE) MRI (A) demonstrates an additional enhancing 6-mm oval mass in the right breast (arrow), assessed as BI-RADS category 4. A circular region of interest (ROI) (shown in red) was drawn on the  $b_{800}$  image (C) and propagated to the other  $b$ -value images (B) and the corresponding apparent diffusion coefficient (ADC) map (D). The ROI appears shifted on the  $b_0$  (B) and ADC map (D), relative to the  $b_{800}$  image (C). This misalignment causes an inaccurate ROI sampling of the lesion, leading to an artifactual increase and decrease in ADC across the lesion on the corresponding ADC map (arrowhead). In general, misregistration errors observed in this study were thought to be caused by subject motion, eddy currents, a shift of the center frequency during the course of the DWI acquisition, or a combination of these factors.



**Table 4.** Factors Associated with Lesion Evaluability

	All Lesions (N = 142)	Non-evaluable Lesions (N = 42)	Evaluable Lesions (N = 100)	PValue
	n (%)	n (%)	n (%)	
Morphology				0.247
Focus	12 (8)	7 (17)	5 (5)	
Mass	73 (51)	20 (48)	53 (53)	
NME	57 (40)	15 (36)	42 (42)	
Lesion size				0.030
≤10 mm	81 (57)	30 (71)	51 (51)	
>10 mm	61 (43)	12 (29)	49 (49)	
DCE-MRI BI-RADS score				0.978
3	30 (21)	9 (21)	21 (21)	
4	105 (74)	31 (74)	74 (74)	
5	7 (5)	2 (5)	5 (5)	
Fat suppression issue				0.732
No	103 (73)	30 (71)	73 (73)	
Yes	39 (27)	12 (29)	27 (27)	
Signal-to-noise ratio issue				0.081
No	111 (78)	28 (67)	83 (83)	
Yes	31 (22)	14 (33)	17 (17)	
Magnetic susceptibility artifact				0.717
No	111 (78)	33 (79)	78 (78)	
Yes	31 (22)	9 (21)	22 (22)	
Aliasing artifact				0.162
No	124 (87)	33 (79)	91 (91)	
Yes	18 (13)	9 (21)	9 (9)	
Misregistration issue				0.001 <sup>a</sup>
No	117 (82)	26 (62)	91 (91)	
Yes	25 (18)	16 (38)	9 (9)	
MRI vendor				0.297
Philips	86 (61)	28 (67)	58 (58)	
Siemens	32 (23)	10 (24)	22 (22)	
GE	24 (17)	4 (10)	20 (20)	
MRI field strength				0.953
1.5 T	55 (39)	16 (38)	39 (39)	
3.0 T	87 (61)	26 (62)	61 (61)	

P values are from the generalized Wald test, using a logistic regression model with generalized estimating equations; percentages may not add up to 100% due to rounding to the nearest integer.

Abbreviations: DCE, dynamic contrast-enhanced; NME, non-mass enhancement.

<sup>a</sup>P value is significant after adjustment for multiple comparisons

measurement, etc.) could allow for more detailed analysis and may provide insights on the impact of various image quality issues affecting multicenter breast DWI. The scan length for the standardized DWI protocol utilized in this study was approximately five minutes, as it included four *b*-values that allowed for both high accuracy in ADC calculation and exploratory analyses of optimal *b*-value combinations. This scan length could be limiting, especially for use in abbreviated MRI protocols that are currently being explored as screening techniques (38). Prior studies, including another secondary analysis of the A6702 study (39) and a breast DWI consensus document have shown that fewer *b*-values do not significantly impact diagnostic performance,

and that two *b*-values is sufficient and reduces scan time to <3 minutes (16,24,40), which would be more appealing for both standard and abbreviated breast MRI protocols.

In conclusion, results from the A6702 multi-institutional study confirmed ADC as a predictive imaging marker of breast malignancy with potential to improve specificity. However, the trial also demonstrated that one-third of the lesions were not evaluable on DWI due to various factors, relating to both image quality and lesion characteristics, that precluded lesion visibility and confident ADC measurement. Results of this secondary analysis highlight that ignoring such image quality issues reduces the diagnostic value of breast DWI. Furthermore, the findings of this trial provide

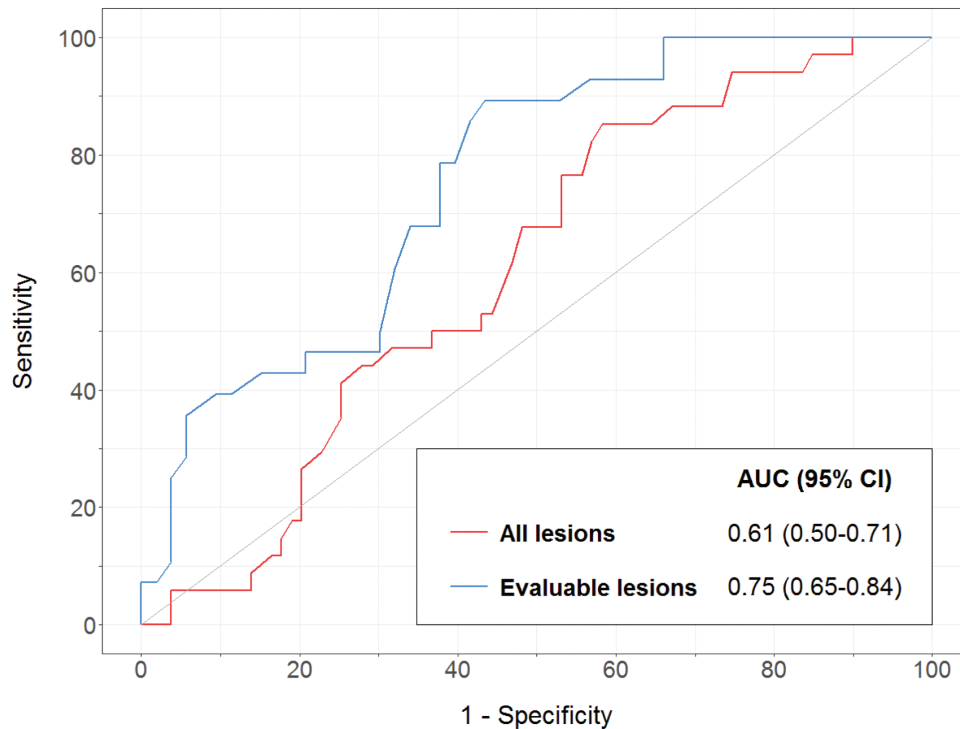


**Figure 8.** Receiver operating characteristic (ROC) curves to predict lesion outcome based on apparent diffusion coefficient (ADC) values. Shown are performance curves based on centrally measured ADC for all lesions (red curve,  $n = 113$ ) and for only the evaluable lesions without significant image quality issues (blue curve,  $n = 81$ ). One of the 114 lesions with reference standard was excluded because it was located outside the DWI slice coverage area. The area under the ROC curve (AUC) is improved when lesions with image quality issues (ie, non-evaluable) are excluded from the analysis (AUC: 0.75 vs. 0.61, respectively).

a roadmap for technical development and standardization efforts of the DWI sequence to allow the full promise of this technology to be widely employed in the clinical setting.

## Acknowledgments

The authors would like to thank the patients for participating in this trial, and the ACRIN 6702 investigators and research staff at all participating sites: University of Washington (Seattle, WA), Vanderbilt University (Nashville, TN), New York University (New York, NY), University of Wisconsin (Madison, WI), MD Anderson Cancer Center (Houston, TX), Northwestern University (Evanston, IL), University of California (San Francisco, CA), Oregon Health Sciences University (Portland, OR), University of Michigan (Ann Arbor, MI), and University of Pennsylvania (Philadelphia, PA).

## Funding

This study was coordinated by the Eastern Cooperative Oncology Group and American College of Radiology Imaging Network Cancer Research Group (Peter J. O'Dwyer, MD and Mitchell D. Schnall, MD, PhD, Group Co-Chairs) and supported by the National Cancer Institute of the National Institutes of Health under the following award numbers: U10CA180820, U10CA180794, U01CA079778, U01CA080098 (to the American College of Radiology Imaging Network), U01CA142565, U01CA166104, R01CA207290,

R01CA203883, U01CA225427, UG1CA233328, UG1CA233270, UG1CA233320, UG1CA233160, UG1CA233329, UG1CA233290, UG1CA233302, and UG1CA233277. The study was also supported by Cancer Prevention and Research Institute of Texas (CPRIT) RR160005 (T.E.Y. is a CPRIT Scholar in Cancer Research). The content is solely the responsibility of the authors and does not necessarily represent the official views of the National Institutes of Health. Mention herein of trade names, commercial products, or organizations does not imply endorsement by the U.S. government.

## Conflict of Interest Statement

E.S.M. disclosed no relevant relationships. J.R. Activities related to the present article: institution received grant from National Cancer Institute. Activities not related to the present article: disclosed no relevant relationships. Other relationships: disclosed no relevant relationships. H.R. Activities related to the present article: institution received grant from National Cancer Institute. Activities not related to the present article: is an uncompensated consultant for Philips Healthcare; has grants/grants pending with GE Healthcare. Other relationships: disclosed no relevant relationships. A.E.K. disclosed no relevant relationships. S.M.H. disclosed no relevant relationships. J.G.W. Activities related to the present article: institution received grant from National Cancer Institute. Activities not related to the present article: receives royalties from Anasys Instruments. Other relationships: disclosed no relevant relationships. T.E.Y. Activities related to the present article: institution received grant from National Cancer Institute. Activities not related to the present article: disclosed

no relevant relationships. Other relationships: disclosed no relevant relationships. L.M. Activities related to the present article: disclosed no relevant relationships. Activities not related to the present article: receives payment from iCAD for board membership; institution has grants/grants pending with Siemens; holds stock/stock options in Lunit. Other relationships: disclosed no relevant relationships. W.B.D. Activities related to the present article: institution received grant from Eastern Cooperative Oncology Group and American College of Radiology Imaging Network. Activities not related to the present article: disclosed no relevant relationships. Other relationships: disclosed no relevant relationships. B.E.D. Activities related to the present article: institution received grant from National Cancer Institute. Activities not related to the present article: is a consultant for Endomag. Other relationships: disclosed no relevant relationships. W.T.Y. Activities related to the present article: disclosed no relevant relationships. Activities not related to the present article: serves on the board of Braid Health; is a consultant for Seno Medical; receives book royalties from Elsevier; receives payment from GE Healthcare for Scientific Advisory Board membership; is a Scientific Advisory Board member for Siemens Medical. Other relationships: disclosed no relevant relationships. L.C.W. disclosed no relevant relationships. B.N.J. disclosed no relevant relationships. L.J.W. disclosed no relevant relationships. N.M.H. Activities related to the present article: institution received grant from Eastern Cooperative Oncology Group and American College of Radiology Imaging Network. Activities not related to the present article: disclosed no relevant relationships. Other relationships: disclosed no relevant relationships. K.Y.O. Activities related to the present article: disclosed no relevant relationships. Activities not related to the present article: institution received U01 grant; received payment for lectures, including service on speakers bureaus; receives royalties from Elsevier. Other relationships: disclosed no relevant relationships. L.A.T. disclosed no relevant relationships. C.H.N. disclosed no relevant relationships. D.I.M. disclosed no relevant relationships. C.E.C. disclosed no relevant relationships. M.D.S. Activities related to the present article: institution received grant from National Institutes of Health. Activities not related to the present article: institution has grants/grants pending with Siemens Healthineers. Other relationships: disclosed no relevant relationships. T.L.C. Activities related to the present article: disclosed no relevant relationships. Activities not related to the present article: disclosed no relevant relationships. Other relationships: is co-inventor of IP assigned to and managed by the University of Michigan (by research agreement, Philips has nonexclusive royalty-free use of this IP; the IP was not used in this study); is co-inventor of IP assigned to and managed by the University of Michigan (ImBio paid license fees to use this IP; the IP is only peripherally related to topic of this work, and ImBio was not a part of this study. ImBio products were not used for this study.) S.C.P. Activities related to the present article: institution received grants from National Institutes of Health and National Cancer Institute. Activities not related to the present article: institution has grants/grants pending with GE Healthcare; institution received in-kind research support from Philips Healthcare. Other relationships: disclosed no relevant relationships.

## References

1. Kuhl C, Weigel S, Schrading S, et al. Prospective multicenter cohort study to refine management recommendations for women at elevated familial risk of breast cancer: the EVA trial. *J Clin Oncol* 2010;28(9):1450–1457.
2. Peters NH, Borel Rinkes IH, Zuithoff NP, Mali WP, Moons KG, Peeters PH. Meta-analysis of MR imaging in the diagnosis of breast lesions. *Radiology* 2008;246(1):116–124.
3. Guo Y, Cai YQ, Cai ZL, et al. Differentiation of clinically benign and malignant breast lesions using diffusion-weighted imaging. *J Magn Reson Imaging* 2002;16(2):172–178.
4. Jiang R, Ma Z, Dong H, Sun S, Zeng X, Li X. Diffusion tensor imaging of breast lesions: evaluation of apparent diffusion coefficient and fractional anisotropy and tissue cellularity. *Br J Radiol* 2016;89(1064):20160076. doi:10.1259/bjr.20160076
5. Yoshikawa MI, Ohsumi S, Sugata S, et al. Relation between cancer cellularity and apparent diffusion coefficient values using diffusion-weighted magnetic resonance imaging in breast cancer. *Radiat Med* 2008;26(4):222–226.
6. Chen L, Liu M, Bao J, et al. The correlation between apparent diffusion coefficient and tumor cellularity in patients: a meta-analysis. *PLoS One* 2013;8(11):e79008. doi:10.1371/journal.pone.0079008
7. White NS, McDonald C, McDonald CR, et al. Diffusion-weighted imaging in cancer: physical foundations and applications of restriction spectrum imaging. *Cancer Res* 2014;74(17):4638–4652.
8. Charles-Edwards EM, deSouza NM. Diffusion-weighted magnetic resonance imaging and its application to cancer. *Cancer Imaging* 2006;6:135–143.
9. Dijkstra H, Dorrius MD, Wielema M, Pijnappel RM, Oudkerk M, Sijens PE. Quantitative DWI implemented after DCE-MRI yields increased specificity for BI-RADS 3 and 4 breast lesions. *J Magn Reson Imaging* 2016;44(6):1642–1649.
10. Parsian S, Rahbar H, Allison KH, et al. Nonmalignant breast lesions: ADCs of benign and high-risk subtypes assessed as false-positive at dynamic enhanced MR imaging. *Radiology* 2012;265(3):696–706.
11. Ei Khoulou RH, Jacobs MA, Mezban SD, et al. Diffusion-weighted imaging improves the diagnostic accuracy of conventional 3.0-T breast MR imaging. *Radiology* 2010;256(1):64–73.
12. Spick C, Pinker-Domenig K, Rudas M, Helbich TH, Baltzer PA. MRI-only lesions: application of diffusion-weighted imaging obviates unnecessary MR-guided breast biopsies. *Eur Radiol* 2014;24(6):1204–1210.
13. Partridge SC, DeMartini WB, Kurland BF, Eby PR, White SW, Lehman CD. Quantitative diffusion-weighted imaging as an adjunct to conventional breast MRI for improved positive predictive value. *AJR Am J Roentgenol* 2009;193(6):1716–1722.
14. Morris EA, Comstock CE, Lee CH, et al. ACR BI-RADS® Magnetic Resonance Imaging. In: *ACR BI-RADS® Atlas, Breast Imaging Reporting and Data System*. Reston, VA: American College of Radiology; 2013.
15. Rahbar H, Zhang Z, Chenevert TL, et al. Utility of diffusion-weighted imaging to decrease unnecessary biopsies prompted by breast MRI: a trial of the ECOG-ACRIN Cancer Research Group (A6702). *Clin Cancer Res* 2019;25(6):1756–1765.
16. Baltzer P, Mann RM, Iima M, et al; EUSOBI international Breast Diffusion-Weighted Imaging working group. Diffusion-weighted imaging of the breast—a consensus and mission statement from the EUSOBI International Breast Diffusion-Weighted Imaging working group. *Eur Radiol* 2020;30(3):1436–1450.
17. RSNA Quantitative Imaging Biomarkers Alliance. QIBA Profile: Diffusion-Weighted Magnetic Resonance Imaging (DWI).

- Available at: <https://qibawiki.rsna.org/index.php/Profiles>. Accessed August 3, 2020.
18. ECOG-ACRIN. A6702: a multi-center study evaluating the utility of diffusion weighted imaging for detection and diagnosis of breast cancer. Protocol and imaging manual. Available at: <https://www.acr.org/Research/Clinical-Research>. Accessed November 3, 2020.
  19. Malyarenko D, Galbán CJ, Londy FJ, et al. Multi-system repeatability and reproducibility of apparent diffusion coefficient measurement using an ice-water phantom. *J Magn Reson Imaging* 2013;37(5):1238–1246.
  20. Stejskal EO, Tanner JE. Spin diffusion measurements: spin echoes in the presence of a time-dependent field gradient. *J Chem Phys* 1965;42:288.
  21. Rahbar H, Kurland BF, Olson ML, et al. Diffusion-weighted breast magnetic resonance imaging: a semiautomated voxel selection technique improves interreader reproducibility of apparent diffusion coefficient measurements. *J Comput Assist Tomogr* 2016;40(3):428–435.
  22. Rutter CM. Bootstrap estimation of diagnostic accuracy with patient-clustered data. *Acad Radiol* 2000;7(6):413–419.
  23. Le Bihan D, Poupon C, Amadon A, Lethimonnier F. Artifacts and pitfalls in diffusion MRI. *J Magn Reson Imaging* 2006;24(3):478–488.
  24. Bogner W, Gruber S, Pinker K, et al. Diffusion-weighted MR for differentiation of breast lesions at 3.0 T: how does selection of diffusion protocols affect diagnosis? *Radiology* 2009;253(2):341–351.
  25. Reese TG, Heid O, Weisskoff RM, Wedeen VJ. Reduction of eddy-current-induced distortion in diffusion MRI using a twice-refocused spin echo. *Magn Reson Med* 2003;49(1):177–182.
  26. Veeraraghavan H, Do RK, Reidy DL, Deasy JO. Simultaneous segmentation and iterative registration method for computing ADC with reduced artifacts from DW-MRI. *Med Phys* 2015;42(5):2249–2260.
  27. Arlinghaus LR, Welch EB, Chakravarthy AB, et al. Motion correction in diffusion-weighted MRI of the breast at 3T. *J Magn Reson Imaging* 2011;33(5):1063–1070.
  28. Bogner W, Pinker-Domenig K, Bickel H, et al. Readout-segmented echo-planar imaging improves the diagnostic performance of diffusion-weighted MR breast examinations at 3.0 T. *Radiology* 2012;263(1):64–76.
  29. Naranjo ID, Lo Gullo R, Morris EA, et al. High-spatial-resolution multishot multiplexed sensitivity-encoding diffusion-weighted imaging for improved quality of breast images and differentiation of breast lesions: a feasibility study. *Radiology: Imaging Cancer* 2020;2(3). doi:10.1148/rycan.2020190076
  30. Barentsz MW, Taviani V, Chang JM, et al. Assessment of tumor morphology on diffusion-weighted (DWI) breast MRI: diagnostic value of reduced field of view DWI. *J Magn Reson Imaging* 2015;42(6):1656–1665.
  31. Hancu I, Lee SK, Hulsey K, et al. Distortion correction in diffusion-weighted imaging of the breast: Performance assessment of prospective, retrospective, and combined (prospective+retrospective) approaches. *Magn Reson Med* 2017;78(1):247–253.
  32. Teruel JR, Fjøsne HE, Østlie A, et al. Inhomogeneous static magnetic field-induced distortion correction applied to diffusion weighted MRI of the breast at 3T. *Magn Reson Med* 2015;74(4):1138–1144.
  33. Newitt DC, Tan ET, Wilmes LJ, et al. Gradient nonlinearity correction to improve apparent diffusion coefficient accuracy and standardization in the american college of radiology imaging network 6698 breast cancer trial. *J Magn Reson Imaging* 2015;42(4):908–919.
  34. Jansen SA, Shimauchi A, Zak L, et al. Kinetic curves of malignant lesions are not consistent across MRI systems: need for improved standardization of breast dynamic contrast-enhanced MRI acquisition. *AJR Am J Roentgenol* 2009;193(3):832–839.
  35. Greenwood HL, Heller SL, Kim S, Sigmund EE, Shaylor SD, Moy L. Ductal carcinoma in situ of the breasts: review of MR imaging features. *Radiographics* 2013;33(6):1569–1588.
  36. Jansen SA, Fan X, Karczmar GS, et al. DCEMRI of breast lesions: is kinetic analysis equally effective for both mass and nonmass-like enhancement? *Med Phys* 2008;35(7):3102–3109.
  37. Ellingson BM, Kim E, Woodworth DC, et al. Diffusion MRI quality control and functional diffusion map results in ACRIN 6677/RTOG 0625: a multicenter, randomized, phase II trial of bevacizumab and chemotherapy in recurrent glioblastoma. *Int J Oncol* 2015;46(5):1883–1892.
  38. Comstock CE, Gatsonis C, Newstead GM, et al. Comparison of abbreviated breast MRI vs digital breast tomosynthesis for breast cancer detection among women with dense breasts undergoing screening. *JAMA* 2020;323(8):746–756.
  39. McDonald ES, Romanoff J, Rahbar H, et al. Mean apparent diffusion coefficient is a sufficient conventional diffusion-weighted MRI metric to improve breast MRI diagnostic performance: results from the ECOG-ACRIN Cancer Research Group A6702 diffusion imaging trial [published online ahead of print November 17, 2020]. *Radiology* 2020. doi:10.1148/radiol.2020202465.
  40. Pereira FP, Martins G, Figueiredo E, et al. Assessment of breast lesions with diffusion-weighted MRI: comparing the use of different b values. *AJR Am J Roentgenol* 2009;193(4):1030–1035.